strategy for neurodegenerative diseases. J Neurochem 114: 1261–1276. PubMed: 20524958.
27. Napoli I, Neumann H (2009) Microglial clearance function in health and disease. Neuroscience 158: 1030–1038. doi:10.1016/j.neuroscience.2008.06.046. PubMed: 18644426.
28. Deshmane SL, Kremlev S, Amini S, Sawaya BE (2009) Monocyte chemoattractant protein-1 (MCP-1): an overview. J Interferon Cytokine Res 29: 313–326. doi:10.1089/jir.2008.0027. PubMed: 19441883.
29. Hickman SE, El Khoury J (2010) Mechanisms of mononuclear phagocyte recruitment in Alzheimer's disease. CNS Neurol Disord Drug Targets 9: 168–173. doi:10.2174/187152710791011982. PubMed: 20205643.
30. Katayama Y, Battista M, Kao WM, Hidalgo A, Peired AJ et al. (2006) Signals from the sympathetic nervous system regulate hematopoietic stem cell egress from bone marrow. Cell 124: 407–421. doi:10.1016/j.cell.2005.10.041. PubMed: 16439213.
31. Ehninger A, Trumpp A (2011) The bone marrow stem cell niche grows up: mesenchymal stem cells and macrophages move in. J Exp Med 208: 421–428. doi:10.1084/jem.20110132. PubMed: 21402747.
32. Lilly AJ, Johnson WE, Bunce CM (2011) The haematopoietic stem cell niche: new insights into the mechanisms regulating haematopoietic stem cell behaviour. Stem Cells Int, 2011: 274564. doi:10.4061/2011/274564. PubMed: 22135682.
33. Méndez-Ferrer S, Lucas D, Battista M, Frenette PS (2008) Haematopoietic stem cell release is regulated by circadian oscillations. Nature 452: 442–447. doi:10.1038/nature06685. PubMed: 18256599.
34. Bradesi S (2010) Role of spinal cord glia in the central processing of peripheral pain perception. Neurogastroenterol Motil 22: 499–511. doi:10.1111/j.1365-2982.2010.01491.x. PubMed: 20236247.
35. Ren K, Dubner R (2010) Interactions between the immune and nervous systems in pain. Nat Med 16: 1267–1276. doi:10.1038/nm.2234. PubMed: 20948535.
36. Viviani B, Bartesaghi S, Gardoni F, Vezzani A, Behrens MM et al. (2003) Interleukin-1beta enhances NMDA receptor-mediated intracellular calcium increase through activation of the Src family of kinases. J Neurosci 23: 8692–8700. PubMed: 14507968.
37. Yang S, Liu ZW, Wen L, Qiao HF, Zhou WX et al. (2005) Interleukin-1beta enhances NMDA receptor-mediated current but inhibits excitatory synaptic transmission. Brain Res 1034: 172–179. doi:10.1016/j.brainres.2004.11.018. PubMed: 15713269.
38. Huang Y, Smith DE, Ibáñez-Sandoval O, Sims JE, Friedman WJ (2011) Neuron-specific effects of interleukin-1β are mediated by a novel isoform of the IL-1 receptor accessory protein. J Neurosci 31: 18048–18059. doi:10.1523/JNEUROSCI.4067-11.2011. PubMed: 22159118.
39. Shaftel SS, Carlson TJ, Olschowka JA, Kyrkanides S, Matousek SB et al. (2007) Chronic interleukin-1beta expression in mouse brain leads to leukocyte infiltration and neutrophil-independent blood brain barrier permeability without overt neurodegeneration. J Neurosci 27: 9301-9309. doi:10.1523/JNEUROSCI.1418-07.2007. PubMed: 17728444.
40. Tsuda M, Tozaki-Saitoh H, Inoue K (2010) Pain and purinergic signaling. Brain. Res Rev 63: 222–232. doi:10.1016/j.brainresrev.2009.11.003.
41. Haynes SE, Hollopeter G, Yang G, Kurpius D, Dailey ME et al. (2006) The P2Y12 receptor regulate s microglial activation by extracellular nucleotides. Nat Neurosci 9: 1512–1519. doi:10.1038/nn1805. PubMed: 17115040.

Am J Physiol Cell Physiol 305: C693–C703, 2013.
First published July 24, 2013; doi:10.1152/ajpcell.00400.2012.

CALL FOR PAPERS *Stem Cell Physiology and Pathophysiology*

Diabetes impairs the interactions between long-term hematopoietic stem cells and osteopontin-positive cells in the endosteal niche of mouse bone marrow

Hironori Chiba,[1] Koji Ataka,[2] Kousuke Iba,[1] Kanna Nagaishi,[2] Toshihiko Yamashita,[1] and Mineko Fujimiya[2]

[1]*Department of Orthopedic Surgery. Sapporo Medical University Faculty of Medicine, Sapporo, Japan, and* [2]*Department of Anatomy, Sapporo Medical University Faculty of Medicine, Sapporo, Japan*

Submitted 10 December 2012; accepted in final form 21 July 2013

Chiba H, Ataka K, Iba K, Nagaishi K, Yamashita T, Fujimiya M. Diabetes impairs the interactions between long-term hematopoietic stem cells and osteopontin-positive cells in the endosteal niche of mouse bone marrow. *Am J Physiol Cell Physiol* 305: C693–C703, 2013. First published July 24, 2013; doi:10.1152/ajpcell.00400.2012.—Hematopoietic stem cells (HSCs) are maintained, and their division/proliferation and quiescence are regulated in the microenvironments, niches, in the bone marrow. Although diabetes is known to induce abnormalities in HSC mobilization and proliferation through chemokine and chemokine receptors, little is known about the interaction between long-term HSCs (LT-HSCs) and osteopontin-positive (OPN) cells in endosteal niche. To examine this interaction, LT-HSCs and OPN cells were isolated from streptozotocin-induced diabetic and nondiabetic mice. In diabetic mice, we observed a reduction in the number of LT-HSCs and OPN cells and impaired expression of Tie2, β-catenin, and N-cadherin on LT-HSCs and β_1-integrin, β-catenin, angiopoietin-1, and CXCL12 on OPN cells. In an in vitro coculture system, LT-HSCs isolated from nondiabetic mice exposed to diabetic OPN cells showed abnormal mRNA expression levels of Tie2 and N-cadherin. Conversely, in LT-HSCs derived from diabetic mice exposed to nondiabetic OPN cells, the decreased mRNA expressions of Tie2, β-catenin, and N-cadherin were restored to normal levels. The effects of diabetic or nondiabetic OPN cells on LT-HSCs shown in this coculture system were confirmed by the coinjection of LT-HSCs and OPN cells into bone marrow of irradiated nondiabetic mice. Our results provide new insight into the treatment of diabetes-induced LT-HSC abnormalities and suggest that the replacement of OPN cells may represent a novel treatment strategy.

osteoblastic niche; Tie2; intrabone marrow-bone marrow transplantation

LONG-LASTING DIABETES IMPAIRS progenitor cell-dependent tissue repair, which is associated with the dysfunction of hematopoietic stem cells (HSCs) in the bone marrow. In type 1 diabetes, progenitor cell-dependent tissue repair is impaired, which is associated with endothelial or hematopoietic progenitor cell dysfunction in the bone marrow (19). The number of Lin^-, $Sca\text{-}1^+$, and $c\text{-}kit^+$ (LSK) hematopoietic progenitor cells in the bone marrow was previously demonstrated to be decreased in streptozotocin (STZ)-induced type 1 diabetic model of mice (7, 27). In the case of type 2 diabetes, the number of bone marrow-derived circulating $CD34^+$ cells was significantly reduced because of the reduced numbers of circulating endothelial progenitor cells. This has been proposed as a mechanism underlying the cardiovascular complications of diabetes (6). Diabetic mice were also shown to have diminished numbers of circulating LSK hematopoietic progenitor cells, leading to delayed wound closure (30).

The involvement of the stem cell niche or bone marrow microenvironment has been proposed as a means of understanding hematopoietic progenitor cell dysfunction (27). Specialized microenvironments (niches) support both self-renewal and the differentiation of HSCs, while their maintenance in a quiescent state is essential to protect them from stress and to sustain long-term hematopoiesis. HSCs are located in the trabecular endosteum (osteoblastic niche) or sinusoidal perivascular area (vascular niche; Ref. 5), the latter including CXCL12-abundant reticular (CAR) cells (26) or $nestin^+$ mesenchymal stem cells (22), which are characterized by high CXCL12 expression (5). In mouse models of diabetes induced by STZ or *db/db*, the CXCL12 mRNA levels in $nestin^+$ cells were reduced, and an impaired interaction between the CXCL12 expressed on $nestin^+$ cells and the HSC-expressed CXCR4 caused poor mobilization of hematopoietic cells after granulocyte colony-stimulating factor (GCSF) treatment (7, 22).

The osteoblastic niche appears to be more involved than the vascular niche in diabetic stem cell abnormalities, because diabetic mice showed significantly reduced numbers of osteoblastic but not $nestin^+$ cells (7). Osteoblasts secrete cytokines/chemokines, including GCSF; granulocyte-macrophage colony-stimulating factor (GM-CSF); macrophage colony-stimulating factor (M-CSF); interleukin (IL)-1, IL-6, and IL-7; and CXCL12, which support HSC survival and differentiation (23). They also express molecules that regulate the HSC numbers, including angiopoietin (Ang), thrombopoietin (TPO), Wnt, Notch, and osteopontin (OPN; Ref. 34), and adhesion molecules including N-cadherin, vascular cell adhesion molecule-1 (VCAM-1), intracellular adhesion molecule-1 (ICAM-1), and annexin II (23). The interaction of HSCs with osteoblastic niche cells through cell adhesion molecules and chemokines and their receptors maintains the balance between cell division/proliferation and quiescence (1).

We previously reported that diabetes induces an increase in the infiltration of bone marrow-derived cells in peripheral organs such as the liver, dorsal root ganglia, and kidney tubulo-interstitial space and that abnormal cell fusion between bone marrow-derived cells and parenchymal cells causes chromosomal abnormalities and accelerates apoptosis in diabetic

Address for reprint requests and other correspondence: M. Fujimiya, Dept. of Anatomy, Sapporo Medical Univ. School of Medicine, South 1, West 17, Chuo-ku, Sapporo 060-8556, Japan (e-mail: fujimiya@sapmed.ac.jp).

animals (4, 9, 31, 36). These findings imply that diabetes primarily leads to a dysfunction of the osteoblastic niche, which subsequently disrupts HSC quiescence and then leads to increased abnormal bone marrow-derived cells, which induce diabetic complications. This hypothesis is supported by the fact that age-dependent hematopoietic dysfunction results mainly from abnormalities in osteoblastic niche cells (21). Mayack et al. (21) reported that young mouse-derived long-term reconstituting HSCs (LT-HSC) cocultured with aged mouse-derived osteoblastic niche cells showed a reduced capacity for hematopoietic reconstitution compared with the young mouse-derived LT-HSCs cocultured with young mouse-derived osteoblastic niche cells. Moreover, the exposure of normal LT-HSCs to aged osteoblastic niche cells is sufficient to worsen the LT-HSC function (21). However, no investigations have been performed to determine whether the exposure of abnormal LT-HSCs to normal osteoblastic niche cells can reverse the LT-HSC abnormalities.

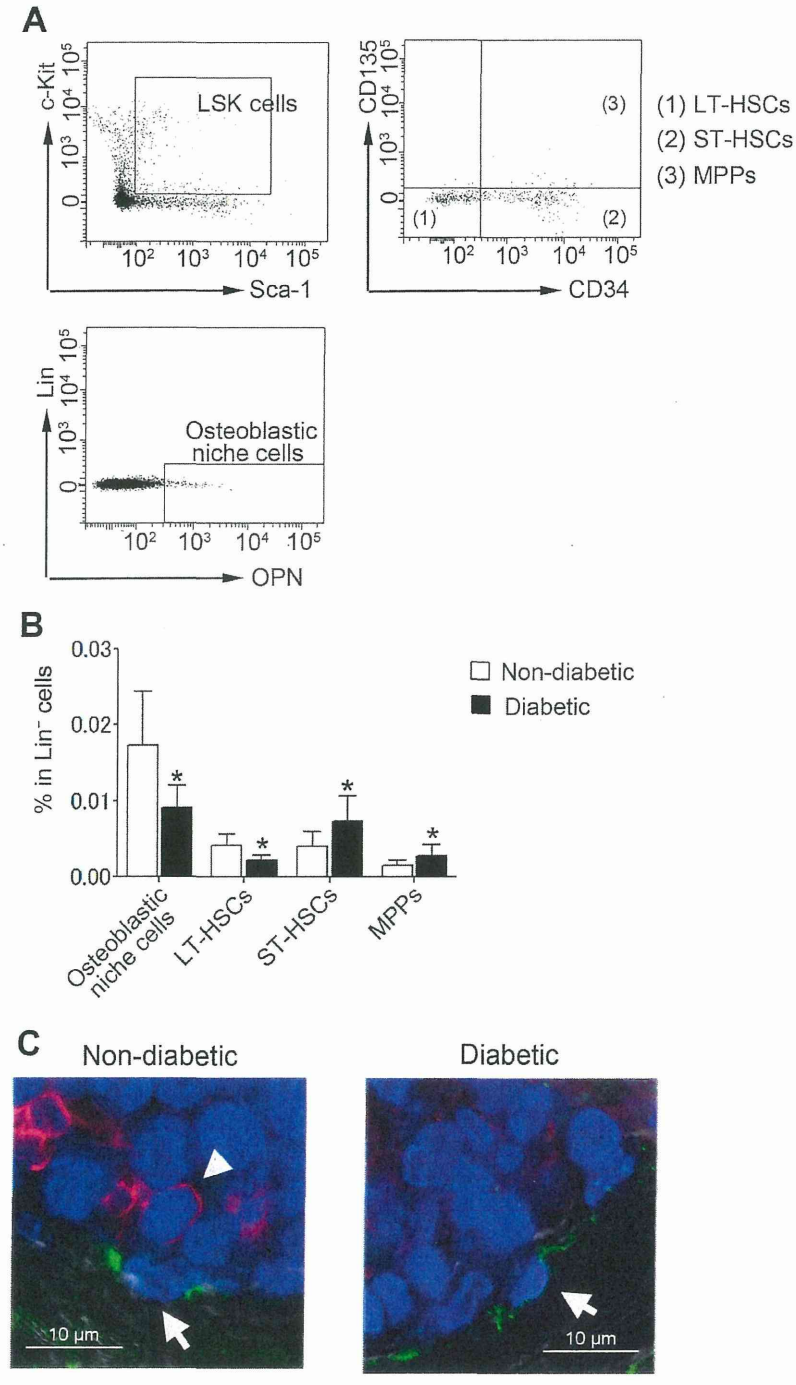

Fig. 1. Isolation of cells from bone marrow. *A*: representative FACS plot of the isolation of long-term hematopoietic stem cells (LT-HSCs; *1*), short-term hematopoietic stem cells (ST-HSCs; *2*), multipotent hematopoietic progenitors (MPPs; *3*), and osteoblastic niche cells. LSK, Lin^-, Sca-1^+, c-kit^+ cells. *B*: cell frequency in Lin^- bone marrow cells. *C*: localization of osteopontin-positive (OPN^+) osteoblastic niche cells (arrow, green) and $CD150^+$ LT-HSCs (arrowhead, red) in the bone marrow. Values are means ± SD for $n = 8$ mice. $^*P < 0.05$, compared with nondiabetic mice.

Therefore, in the present study, we performed in vivo experiments to examine whether diabetes induces the abnormal expression of molecules that are essential for maintaining the quiescence and reconstitution of HSCs in the bone marrow niche. Using in vitro coculture experiments, we also examined whether exposure of normal LT-HSCs to diabetic osteoblastic niche cells induced the abnormal expression of molecules on LT-HSCs seen in the in vivo experiments. We further examined whether the abnormal expression of molecules on diabetic LT-HSCs could be reversed following exposure to normal osteoblastic niche cells. Finally, these results obtained from in vitro studies were confirmed by intrabone marrow-bone marrow transplantation (IBM-BMT) with the replacement of osteoblastic niche cells and the effects on the LT-HSCs were examined.

MATERIALS AND METHODS

Animal studies. C57BL/6 male mice were purchased from the Sankyo Laboratory (Tokyo, Japan). Diabetes was induced by a single intraperitoneal injection of 150 mg/kg STZ dissolved in citrate buffer (pH 4.5) into 8- to 10-wk-old mice. Four weeks after the injection, the blood glucose levels were assayed, and mice with blood glucose concentrations >400 mg/dl were used in the present study. Nondiabetic control mice were injected with 100 μl of vehicle. All animal experiments were approved by the Animal Use Committee of Sapporo Medical University, Sapporo, Hokkaido, Japan.

Flow cytometry. LT-HSCs and osteoblastic niche cells were sorted as LSK $CD135^-$ $CD34^-$ cells and Lin^- OPN^+ cells, respectively (21). The femora and tibiae of four mice treated with vehicle or STZ were crushed and digested at 37°C for 1 h with Hanks' buffered saline including 0.25% trypsin, 1 mM EDTA (25200; Life Technologies, Grand Island, NY), and 0.1% collagenase (034–10533; WAKO, Osaka, Japan). Cells were washed with phosphate-buffered saline (pH 7.5) containing 2% FCS and were filtered through a 40-μm cell strainer filter (BD Biosciences, Franklin Lakes, NJ). Erythrocytes were lysed using ammonium chloride potassium lysis buffer (Qiagen, Tokyo, Japan). Cell suspensions were incubated with a biotinylated lineage cocktail [anti-CD5, anti-CD45R (B220), anti-CD11b, anti-Gr-1 anti-Ly-6G/C, and anti-Ter-119; 130–090-858; Miltenyi Biotec, Auburn, CA], followed by anti-biotin MicroBeads (130–090-485; Miltenyi Biotec). Lin^- cells were isolated with a MACS column and separator (Miltenyi Biotec) and stained with anti-c-Kit-APC-Cy7 (2B8; BD Biosciences), anti-Sca-1-PE-Cy7 (D7; Biolegend, San Diego, CA), anti-CD34-Alexa Flour 700 (RAM34; BD Biosciences), anti-CD135-PE (A2F10; Biolegend), or anti-OPN (18621; Immuno-Biological Laboratories, Gunma, Japan) antibody. Anti-rabbit IgG-conjugated APC (R&D Systems, Minneapolis, MN) was used as the anti-OPN secondary antibody. A DAPI solution (D523; DOJINDO, Kumamoto, Japan) was used to exclude dead cells. LSK cells were sorted first, and the LSK cells were subsequently isolated using CD135 and CD34 antibodies (Fig. 1*A*). $CD135^-$ $CD34^-$ cells were identified as LT-HSCs, $CD135^-$ $CD34^+$ cells as short-term reconstituting HSCs (ST-HSCs), and $CD135^+$ $CD34^+$ cells as multipotent hematopoietic progenitors (MPPs; Fig. 1*A*). Lin^- OPN^+ cells were identified as osteoblastic niche cells (Fig. 1*A*). After coculture experiments, the culture medium was discarded, and adherent cells were removed using Hanks' buffered saline including 0.25% trypsin and 1 mM EDTA for 15 min. Sorting of LT-HSCs and osteoblastic niche cells was carried out by FACS as described above.

Osteoblastic niche cells and LT-HSCs coculture. To investigate the interactions between LT-HSCs and osteoblastic niche cells, we cocultured sorted LT-HSCs (6×10^3 cells) and osteoblastic niche cells (6×10^4 cells) with DMEM supplemented with 10% FBS, 1% penicillin, 150 ng/ml Fms-like tyrosine kinase 3 (FLT3) ligand, 150 ng/ml stem cell factor (SCF), and 150 ng/ml TPO at the glucose concentrations of 100 mg/dl for the normal glucose medium or 450 mg/dl for the high-glucose medium. Osteoblastic niche cells and LT-HSCs were seeded at the same time in 16-well chamber slides (Thermo Scientific, Barrington, IL) at 37°C in 5% CO_2-air for 7 days. On *day 3*, the culture medium was changed. The cocultured cell morphology was observed under phase-contrast microscopy.

HSC differentiation and the colony-forming assay. To examine the hematopoiesis potential of the hematopoietic cells, LSK cells were sorted from the femora and tibiae of vehicle and STZ-injected mice by FACS and cultured in CytoSelect Methylcellulose Medium (CBA-320; Cell Biolabs) containing 10% FBS, 500-ng/ml SCF, 100-ng/ml IL-3, 100-ng/ml GM-CSF, and 30-ng/ml erythropoietin (Ep) at 5% CO_2-air and 37°C for 7 days (25). Colony formation was measured with CyQuant GR dye solution (CBA-320; Cell Biolabs). The number of sorted LSK cells was counted by FACS.

Serum TRAP5b assay. To compare the bone resorption activity of the osteoclasts in vehicle- and STZ-injected mice, blood was collected

Table 1. *Primer sequences for PCR*

Protein	Primer Sequence
N-cadherin	
F	5′-AATCAGACGGCTAGACGAGAGG-3′
R	5′-TCAGCAGATTTAAGGCCCTCAT-3′
β-Catenin	
F	5′-ACGCGTGTGAGAAAGAATACAGAC-3′
R	5′-GCTTGAGTTTGGTTCTGGGC-3′
β_1-Integrin	
F	5′-TGGAAAATTCTGCGAGTGTGAT-3′
R	5′-TGCCAGTGTAATTGGGATAGCA-3′
Wnt10b	
F	5′-GCGAAGGATAATAGCAGGCAT-3′
R	5′-TTGTCACCCGAGGTCCCATA-3′
Dkk1	
F	5′-CAAAAATGTATCACACCAAAGGACAA-3′
R	5′-TGCTTGGTACACACTTGACCT-TCTT-3′
Fzd4	
F	5′-GTGGATGCCGATGAACTGAC-3′
R	5′-ACAGCGTTCCAATCACCAAA-3′
Fzd7	
F	5′-TATCGCCTACAACCAGACCATC-3′
R	5′-GGGTGCGTACATAGAGCATAAGA-3′
LRP5	
F	5′-CCCACTCACGGGTGTCAAA-3′
R	5′-TGCTCCACTGAGCTCCCATT-3′
LRP6	
F	5′-TGGCTTGGCGGTGTGAT-3′
R	5′-CACACGGGACAATTGAGTTCA-3′
Ang-1	
F	5′-CAGCACGAAGGATGCTGATAAC-3′
R	5′-TTGTCCCGCAGTGTAGAACATT-3′
Tie2	
F	5′-AAGCATGCCCATCTGGTTAC-3′
R	5′-GCCTGCCTTCTTTCTCACAC-3′
CXCL12	
F	5′-GCTCTGCATCAGTGACGGTA-3′
R	5′-TAATTACGGGTCAATGCACA-3′
CXCR4	
F	5′-CTTTGTCATCACACTCC-CCTT-3′
R	5′-GCCCACATAGACTGCCT-TTTC-3′
TPO	
F	5′-CCAGACGGAACAGAGCAAG-3′
R	5′-CTGTCCTCGTGCTGCCAT-3′
MPL	
F	5′-CCTGCACTGGAGGGAGGTCT-3′
R	5′-GGCTCCAGCACCTTCCAGTC-3′
GAPDH	
F	5′-CTACAGCAACAGGGTGGTGGAC-3′
R	5′-GGATAGGGCCTCTCTTGCTCAG-3′

F, forward; R, reverse.

and centrifuged at 300 *g* for 10 min, and the level of serum tartrate-resistant acid phosphatase (TRAP) 5b was measured using a mouse TRAP assay kit (SB-TR10; Immunodiagnostic Systems).

Measurements of the length and weight of femora. The femora were isolated from six to seven mice that were treated with vehicle or STZ, and the length and weight were measured.

Immunofluorescence staining for bone marrow sections. Mice were anesthetized with pentobarbital and perfused with 4% paraformaldehyde in phosphate buffer. Isolated bones were decalcified with decalcifying solution B (041–22031; WAKO), and cryostat-cut sections were prepared using adhesive film (14). Sections were blocked with 2% goat serum and incubated in rabbit anti-mouse OPN (ab8448; Abcam, Cambridge, UK) and PE-conjugated rat anti-mouse CD150 antibodies (115904; BioLegend) or sheep anti-mouse CD150 (AF4330; R&D Systems), a maker of LT-HSC (35), rat anti-mouse Tie2 (124002; BioLegend), and Pacific Blue conjugated anti-mouse lineage cocktail (133310; BioLegend) and were further incubated in Texas Red-labeled goat anti-rabbit IgG (TI-1000; Vector Laboratories), Cy3 donkey anti-sheep IgG (713–165-003; Jackson Laboratories), Alexa Fluor 647 goat anti-rat IgG (112–605-003; Jackson Laboratories), and Alexa Fluor 488 goat anti-rabbit IgG (711–544-152; Jackson Laboratories) as a secondary antibody.

Immunofluorescence staining of cultured cells. A morphological analysis of coculture cells labeled with different color of fluorescence was performed. Isolated LT-HSCs were incubated at 37°C for 1 h with the culture medium containing Qtracker 525 (Invitrogen) and then were cocultured with isolated osteoblastic niche cells at 37°C in 5%CO_2-air for 1 wk. On *day 7*, the cocultured cells were fixed with 4% paraformaldehyde in PBS, incubated with 2% BSA in PBS and stained with anti-OPN (1:50; Immuno-Biological Laboratories) in PBS containing 0.25% Triton X-100. Anti-rabbit IgG-conjugated Cy5 (1:500; ab6564; Abcam) was used as a secondary antibody. Nuclei were stained with DAPI. Fluorescence images were obtained under a confocal laser microscope (A1; Nikon, Tokyo, Japan).

Quantitative RT-PCR analysis. To examine the mRNA expression of various targets, total RNA was extracted using the RNeasy Plus Micro Kit (Qiagen), and cDNA was synthesized using the SuperScript First-Strand Synthesis System for RT-PCR (Invitrogen, Grand Island, NY). Quantitative RT-PCR for N-cadherin, β-catenin, β_1-integrin, Tie2, CXCR4, Frizzled (Fzd) receptor4, Fzd7, lipoprotein receptor-related protein 5 (LRP5), LRP6, thrombopoietin receptor (MPL), Ang-1, CXCL12, wingless-type MMTV integration site family, member 10b (Wnt10b), dickkopf-1 (Dkk1), and TPO was performed on the ABI prism 7500 Sequence Detection System (Applied Biosystems; Foster City, CA) with Power SYBR GREEN PCR Master Mix (4367659; Applied Biosystems). The relative mRNA expression was quantified by the $^{2-}\Delta C_T$ method. The primer sequences are shown in the Table 1.

IBM-BMT. To evaluate the interaction of LT-HSCs and osteoblastic niche cells in vivo, OPN^+ cells and OPN^- cells, in which LT-HSCs were included, were transplanted into bone marrow as follows: OPN^+ and OPN^- cells were sorted from the femora and tibiae of vehicle- or STZ-injected mice by MACS. Mice were irradiated (10 Gy) and transplanted with the mixture of 2×10^6 OPN^+ and 1.5×10^4 OPN^- cells derived from either diabetic or nondiabetic mice via IBM-BMT 1 day

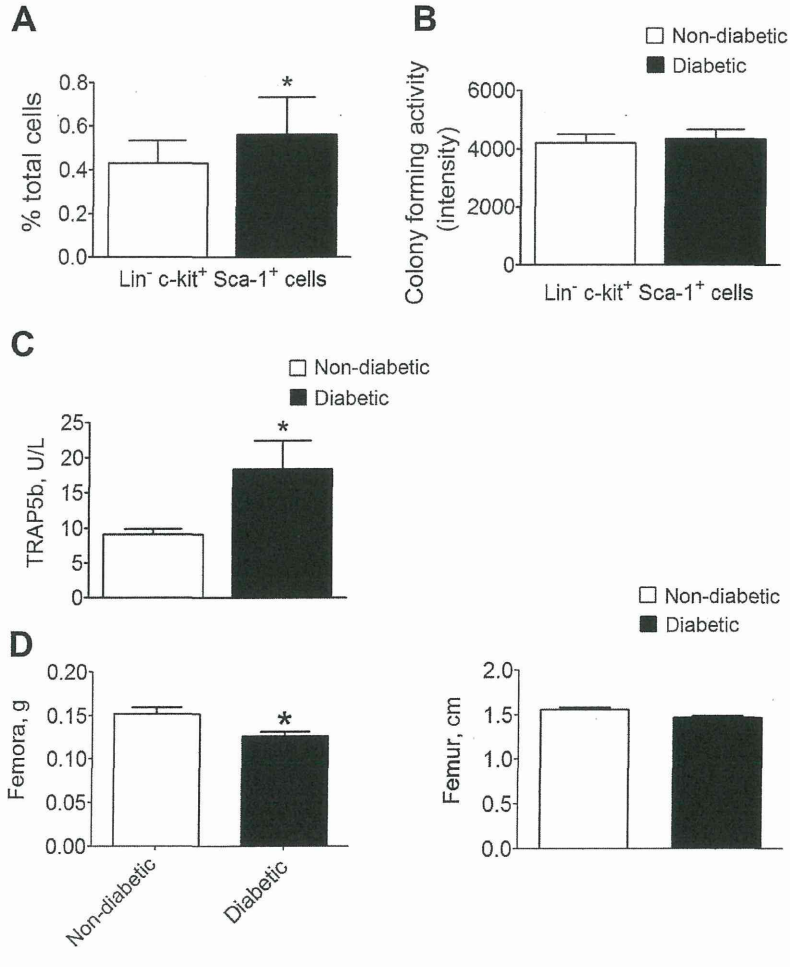

Fig. 2. Activity of Lin^-, $Sca\text{-}1^+$, and $c\text{-}kit^+$ (LSK) cells. *A*: frequency of LSK cells in mononuclear cells as determined by FACS. *B*: HSC colony-forming activity. *C*: TRAP5b activity. *D*: weight of femora and length of the femur. Values are the means ± SD for $n = 4-6$ mice. $^*P < 0.05$, compared with nondiabetic mice.

after the irradiation according to a previously study (16). One week after the bone marrow transplantation, LT-HSCs were sorted by FACS as described above, and the mRNA expression of Tie2 was examined.

Statistical analysis. Differences between groups were determined using a two-tailed Student's *t*-test and one-way ANOVA, followed by a Tukey's multiple comparison test. Differences were considered significant for values of $P < 0.05$.

RESULTS

Frequency of osteoblastic niche cells, LT-HSCs, ST-HSCs, and MPPs in diabetic and nondiabetic mouse bone marrow. The percentages of osteoblastic niche cells, LT-HSCs, ST-HSCs, and MPPs in Lin$^-$ bone marrow cells were compared, and the osteoblastic niche cells and LT-HSCs were both shown

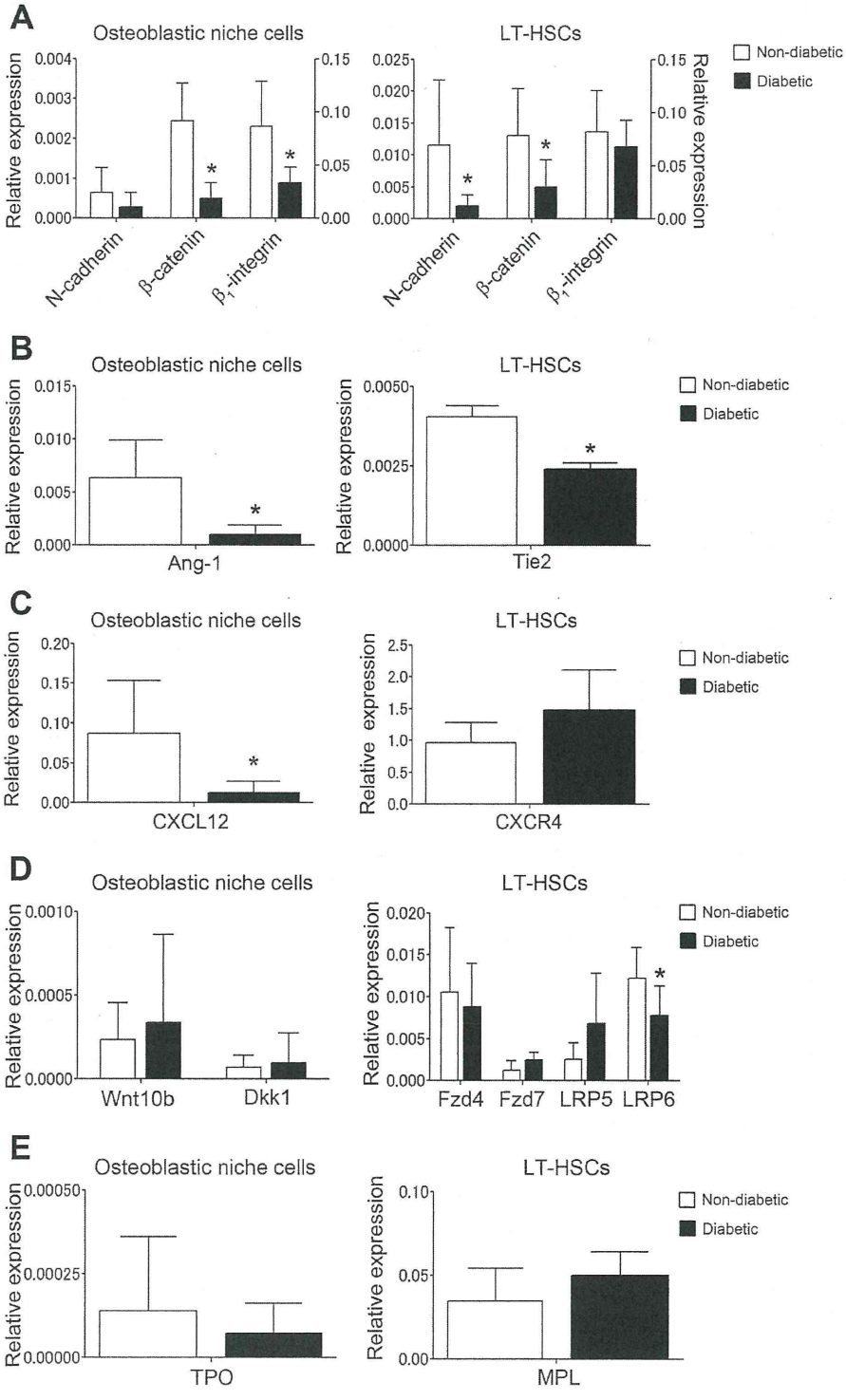

Fig. 3. Comparison of the expression levels of various molecules. *A*: expression of N-cadherin (*left axis*), β-catenin (*middle axis*), and β_1-integrin (*right axis*) on osteoblastic niche cells and LT-HSCs. *B*: expression of angiopoietin-1 (Ang-1) and Tie2. *C*: expression of CXCL12 and CXCR4. *D*: expression of proteins related to Wnt/β-catenin signaling pathways. *E*: expression of thrombopoietin (TPO) and thrombopoietin receptor (MPL). Values are the means ± SD for $n = 6-8$ mice. *$P <$ 0.05, compared with nondiabetic mice.

to be significantly reduced, while ST-HSCs and MPPs were significantly increased in diabetic mice compared with nondiabetic mice (Fig. 1*B*).

Localization of osteoblastic niche cells and LT-HSCs in diabetic and nondiabetic mouse bone marrow. The in vivo localization of osteoblastic niche cells and LT-HSCs in the bone marrow of diabetic and nondiabetic mice was examined by immunofluorescence staining (Fig. 1*C*). OPN^+ osteoblastic niche cells were located at the endosteum in both diabetic and nondiabetic mice (green color, arrows), and CD150-positive LT-HSCs were located adjacent to osteoblastic niche cells (red color, arrowheads).

Functional abnormalities in the HSCs from diabetic mice. To compare the hematopoiesis differentiation potentials of HSCs between diabetic and nondiabetic mice, we performed colony-forming assays on LSK cells. The number of LSK cells from the diabetic mice was significantly increased compared with that in the nondiabetic mice; however, the intensity of colony formation of differentiated cells, including neutrophil, macrophage, eosinophil, erythrocyte, and megakaryocyte from LSK cells induced by SCF, IL-3, GM-CSF, and Ep was not significantly different between diabetic and nondiabetic mice (Fig. 2, *A* and *B*). The activity of osteoclasts derived from hematopoietic progenitors was also compared between the

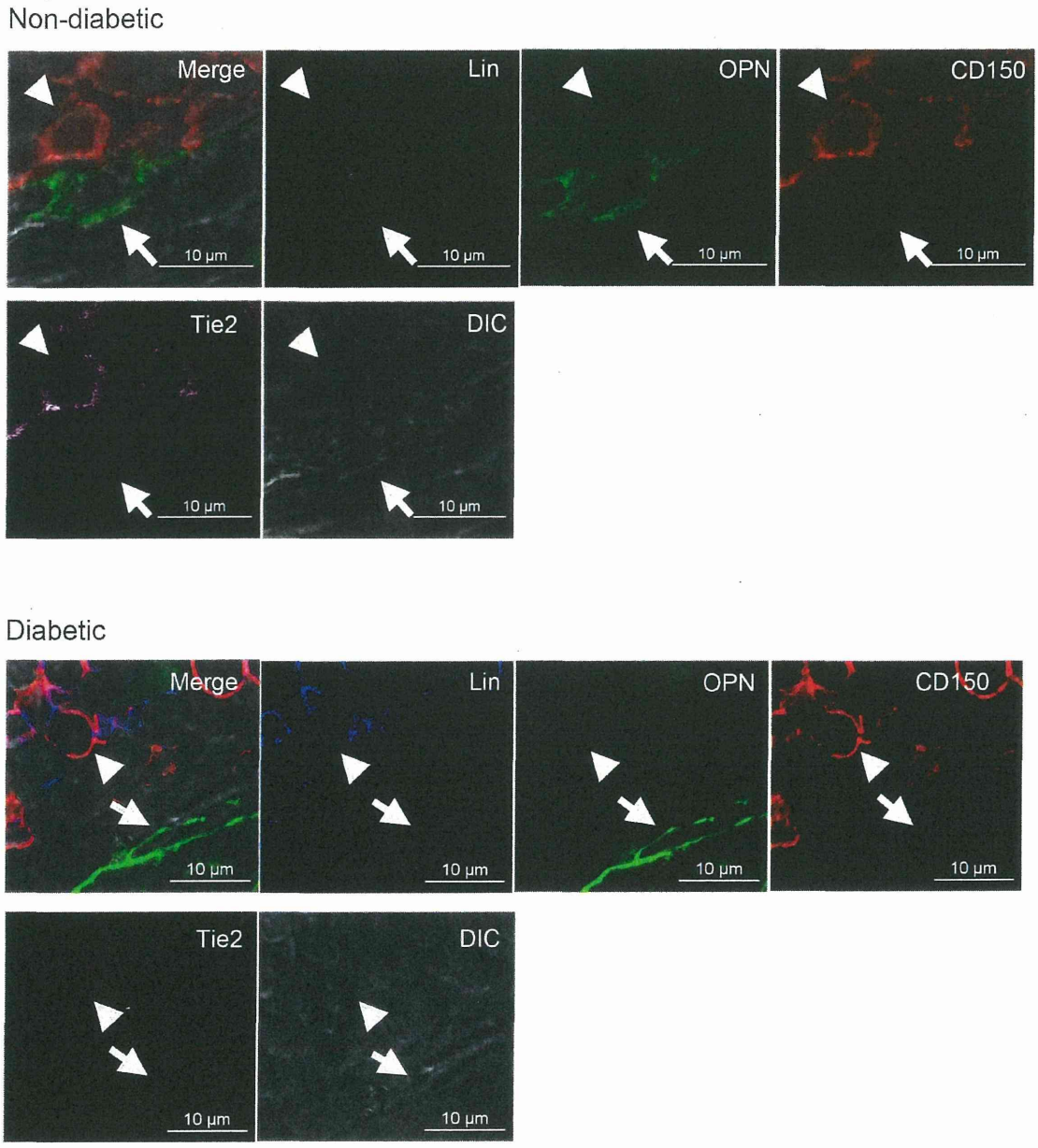

Fig. 4. Immunofluorescence staining of OPN^+ (green) osteoblastic niche cell (arrow) and $CD150^+$ (red) LT-HSCs (arrowhead). Lin^- $CD150^+$ LT-HSC is stained with Tie 2 (pink) in nondiabetic mice; however, the intensity of Tie 2 immunoreactivity is dramatically decreased in diabetic mice.

diabetic and nondiabetic mice. TRAP5b, indicating the bone resorption activity of osteoclasts, was significantly increased in diabetic mice compared with nondiabetic mice (Fig. 2*C*). The length of the femur was not significantly different between diabetic and nondiabetic mice; however, the weight of the femora of diabetic mice was lower than that of the nondiabetic mice (Fig. 2*D*).

Expression of osteoblastic niche cell- and LT-HSC-related molecules in diabetic and nondiabetic mouse bone marrow. The expression of cell adhesion molecules such as N-cadherin, β-catenin, and β_1-integrin on isolated osteoblastic niche cells and LT-HSCs from diabetic mice was compared with that from nondiabetic mice. The expression of β-catenin and β_1-integrin on isolated osteoblastic niche cells was significantly reduced in diabetic mice, but the expression of N-cadherin was unchanged (Fig. 3*A*). Diabetic mice showed significantly reduced N-cadherin and β-catenin expression on LT-HSCs compared with nondiabetic mice, while the expression of β_1-integrin on LT-HSCs was unchanged (Fig. 3*A*). The Ang-1 expression on the osteoblastic niche cells from diabetic mice was also significantly reduced compared with that from nondiabetic mice, and the expression of the Ang-1 ligand, Tie2, on LT-HSCs was also significantly reduced in diabetic mice (Fig. 3*B*). The CXCL12 expression on osteoblastic niche cells was significantly reduced in diabetic mice, but the expression of its receptor, CXCR4, was unchanged on LT-HSCs (Fig. 3*C*). In terms of the Wnt/β-catenin signaling pathways, neither the Wnt 10b expression on osteoblastic niche cells nor the expression of receptors for Wnt family proteins, such as Fzd4, Fzd7, and LRP5, on LT-HSCs was changed; however, the LRP6 expression on LT-HSCs was reduced in diabetic mice (Fig. 3*D*). The Dkk1 expression was the same on osteoblastic niche cells from both diabetic and nondiabetic mice (Fig. 3*D*), as was the expression of TPO on osteoblastic niche cells, and the expression of its receptor, MPL, on LT-HSCs (Fig. 3*E*). In the immunohistochemical analysis for Tie 2 expression, the intensity of $Tie2^+$ immunoreactivity was dramatically decreased on Lin^- CD 150^+ LT-HSC cells in diabetic mice compared with nondiabetic mice (Fig. 4). A summary of these results is shown in Fig. 5.

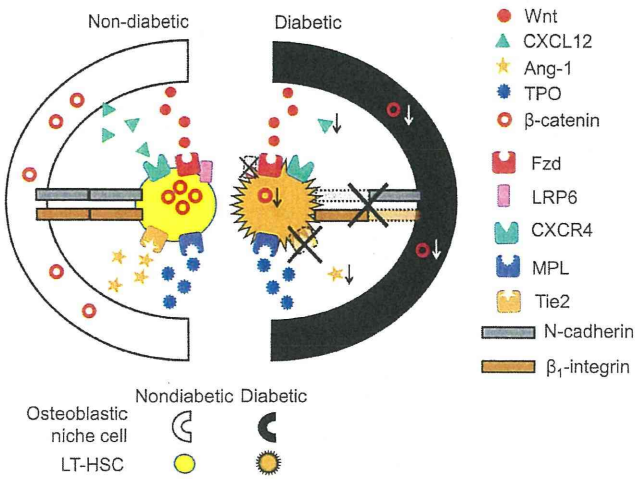

Fig. 5. Summary of the expression of molecules on osteoblastic niche cells and LT-HSCs derived from diabetic and nondiabetic mice.

In vitro coculture of osteoblastic niche cells and LT-HSCs to mimic the bone marrow microenvironment in diabetic and nondiabetic mice. We performed in vitro coculture experiments using LT-HSCs and osteoblastic niche cells derived from diabetic and nondiabetic mice. We used the 450-mg/dl (25 mM) glucose concentration as the high-glucose medium and 100-mg/dl (5.6-mM) concentration as the normal glucose medium because in the present study the blood glucose levels in diabetic and nondiabetic mice were 730.9 ± 135.6 and 167.25 ± 42.4 mg/dl, respectively (n = 15). In previous in vitro study, 5.5 and 33 mM were used as the normal and high-glucose media, and 27 mM glucose concentration was used to evaluate the effects of glucose on transplanted β-cells as an in vitro diabetic condition (20, 32). After 7 days in coculture, LT-HSCs were found to be in contact with the osteoblastic niche cells at the bottom of the culture plates (Fig. 6, *Aa* and *Ab*). These adherent cells were collected and subsequently isolated into LT-HSCs and osteoblastic niche cells by FACS. As shown in Fig. 6*B*, osteoblastic niche cells derived from nondiabetic mice were still adherent to the bottom in normal glucose medium but lost their adherence in the high-glucose medium (Fig. 6, *Ba* and *Bb*). On the other hand, the osteoblastic niche cells derived from diabetic mice were adherent in the high-glucose medium but in the normal glucose medium (Fig. 6, *Bc*−*Bf*). However, osteoblastic niche cells derived from nondiabetic mice that were cocultured with LT-HSCs derived from diabetic mice adhered to the bottom even in the high-glucose medium (Fig. 6*Bh′*). The survival frequency of LT-HSCs paralleled the existence of osteoblastic niche cells (Fig. 6, *Ba′*−*Bh′*), and LT-HSCs survived in a 7-day coculture system in cases where the osteoblastic niche cells were adherent to the bottoms of the wells (Fig. 6, *Ba′*, *Bd′*, *Bf′*, *Bg′*, and *Bh′*).

Changes in the expression of molecules on LT-HSCs cocultured with osteoblastic niche cells. The expression of molecules on LT-HSCs derived from diabetic or nondiabetic mice was examined after coculture with osteoblastic niche cells derived from diabetic or nondiabetic mice in different glucose conditions. This analysis was only carried out in cases where cells were detected after a 7-day coculture as shown in Fig. 6, *Ba′*, *Bd′*, *Bf′*, *Bg′*, and *Bh′*. We analyzed the N-cadherin, β-catenin, and Tie2 expression on LT-HSCs, as these were shown to be reduced in the in vivo diabetic model mice. N-cadherin expression on diabetic LT-HSCs exposed to diabetic osteoblastic niche cells was significantly reduced compared with that on nondiabetic LH-HSCs exposed to nondiabetic osteoblastic niche cells (Fig. 7, *Aa* and *Ab*). This was also observed for N-cadherin expression on nondiabetic LT-HSCs exposed to diabetic osteoblastic niche cells under high-glucose concentrations compared with those exposed to nondiabetic osteoblastic niche cells (Fig. 7, *Aa* and *Ac*). However, the reduced expression of N-cadherin on diabetic LT-HSCs exposed to diabetic osteoblastic niche cells (Fig. 7*Ab*) was reversed after exposure to nondiabetic osteoblastic niche cells under either normal or high-glucose conditions (Fig. 7, *Ad* and *Ae*). Similarly, the β-catenin expression on LT-HSCs was examined after in vitro coculture with osteoblastic niche cells. The β-catenin expression on diabetic LT-HSCs exposed to diabetic osteoblastic niche cells was significantly reduced compared with that on nondiabetic LH-HSCs exposed to nondiabetic osteoblastic niche cells (Fig. 7, *Ba* and *Bb*). This was reversed after exposure to nondiabetic osteoblastic niche cells

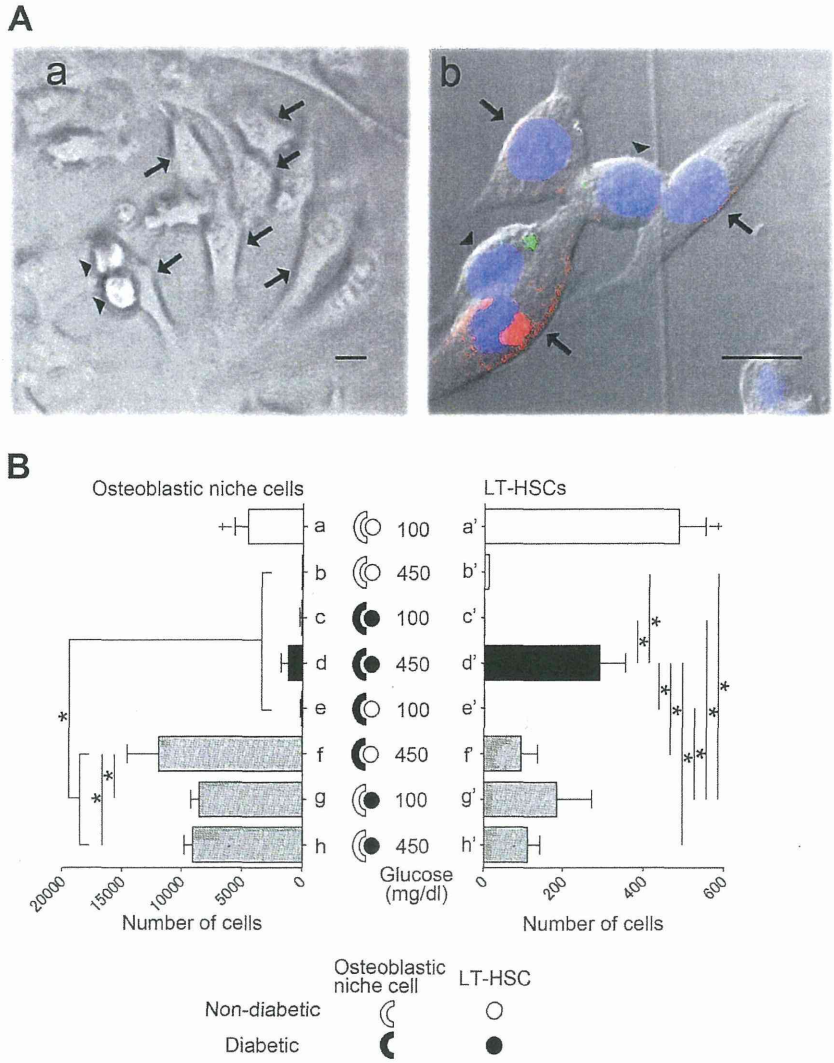

Fig. 6. Findings of the in vitro coculture studies. *Aa*: Phase-contrast microscopy of osteoblastic niche cells (arrows) and LT-HSCs (arrowheads) on *day 7*. Scale bar = 10 μm. *Ab*: Qtracker 525 (green) was detected in the cytoplasm of LT-HSCs (arrow heads) and an OPN-positive reaction (red) was seen in the cytoplasm of osteoblastic niche cells (arrows). Scale bar = 10 μm. *B*: numerical comparison of osteoblastic niche cells and LT-HSCs derived from diabetic and nondiabetic mice cocultured under normal (100 mg/dl) and high glucose (450 mg/dl) conditions. Values are the means ± SD for $n = 6-8$ mice. $*P < 0.05$ and $\dagger P < 0.05$, compared with other groups.

under normal glucose concentrations (Fig. 7*Bd*). The Tie2 expression on diabetic LT-HSCs exposed to diabetic osteoblastic niche cells was significantly reduced compared with that on nondiabetic LH-HSCs exposed to nondiabetic osteoblastic niche cells (Fig. 7, *Ca* and *Cb*). This was reversed after exposure to nondiabetic osteoblastic niche cells under normal glucose concentrations (Fig. 7*Cd*). The Tie2 expression on nondiabetic LT-HSCs cocultured with diabetic osteoblastic niche cells under high-glucose concentrations was also significantly reduced compared with those exposed to nondiabetic osteoblastic niche cells (Fig. 7, *Ca* and *Cc*).

IBM-BMT for in vivo replacement of osteoblastic niche cells. To confirm the findings obtained from in vitro coculture experiments, we performed IBM-BMTs using OPN^+ and OPN^- cells in different combinations as follows: nondiabetic OPN^+ with nondiabetic OPN^- (Fig. 8*a*), diabetic OPN^+ with diabetic OPN^- (Fig. 8*b*), diabetic OPN^+ with nondiabetic OPN^- (Fig. 8*c*) and nondiabetic OPN^+ with diabetic OPN^- cells (Fig. 8*d*). One week after the bone marrow transplantation, the message level of Tie2 on LT-HSCs was examined. The results showed that the reduced expression of Tie2 on diabetic LT-HSCs exposed to diabetic osteoblastic niche cells (Fig. 8*b*) was completely revered by exposure to nondiabetic osteoblastic niche cells (Fig. 8*d*). On the other hand, the Tie2 expression on nondiabetic LT-HSCs was significantly reduced by exposure to the diabetic osteoblastic niche cells (Fig. 8*c*).

DISCUSSION

Most LT-HSCs are located at the trabecular bone surface of the bone marrow, and their interaction with osteoblastic cells through signaling and cell adhesion molecules appears to be essential to sustain their quiescence and preserve the self-renewal of stem cells during normal hematopoiesis (18). While long-term diabetes is known to impair the mobilization of hematopoietic progenitor cells (7, 22) or diminish the total number of HSCs in both human and mice, few studies have examined the interaction between HSCs and osteoblastic niche cells under diabetic conditions.

In the present study, we isolated LT-HSCs (LSK, $CD34^-$, and $CD135^-$) and osteoblastic niche cells (Lin^- and OPN^+)

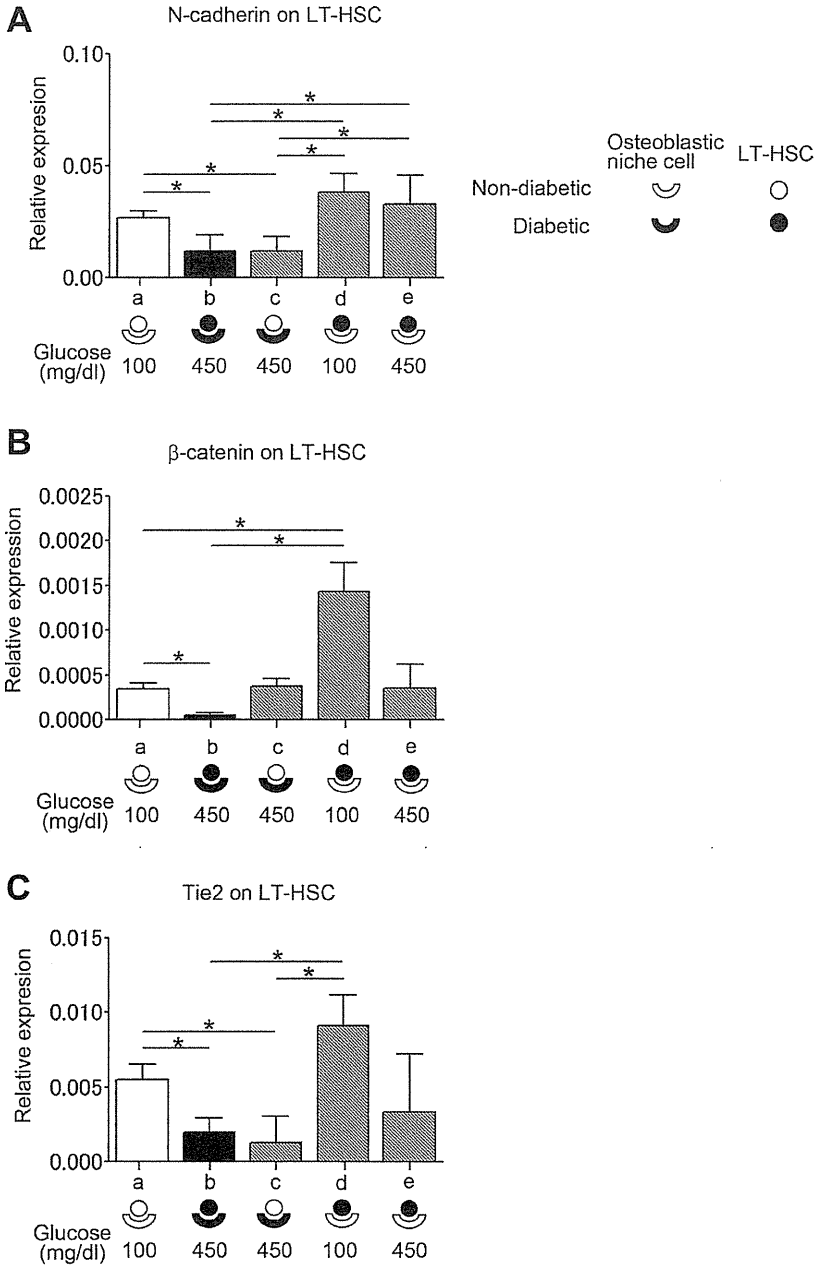

Fig. 7. Expression of molecules on LT-HSCs cocultured with osteoblastic niche cells. mRNA expression levels of N-cadherin (*A*), β-catenin (*B*), and Tie2 (*C*) on nondiabetic (*a* and *c*) or diabetic (*b*, *d*, and *e*) LT-HSCs cocultured with nondiabetic (*a*, *d*, and *e*) or diabetic (*b* and *c*) osteoblastic niche cells cultured under normal (100 mg/dl)- and high (450 mg/dl)-glucose conditions. Values are the means ± SD for $n = 6-8$ mice. $^*P < 0.05$, compared with other groups.

from the bone marrow of mice with and without diabetes and examined the expression of molecules that regulate the quiescence, apoptosis, and cell adhesion to maintain hematopoietic reconstitution.

FACS analysis showed that the numbers of osteoblastic niche cells and LT-HSCs were reduced, while those of ST-HSCs and MPPs were increased in diabetic mice. Because the numbers of osteoblastic niche cells and LT-HSCs are correlated, the depletion of the former may be caused by depletion of the latter. The observed increase in ST-HSCs and MPPs suggests that, in diabetes, the osteoblastic niche cells fail to maintain the LT-HSCs quiescent, so that their differentiation into ST-HSCs and MPPs was accelerated. Further evidence for this came from the observation that the Ang-1 expression on osteoblastic niche cells and Tie2 expression on HSCs was reduced in diabetic mice. Ang-1 is produced mainly by osteoblastic niche cells, and its receptor tyrosine kinase, Tie2, is expressed on LT-HSCs. Tie2/Ang-1 signaling promotes the tight adhesion of HSCs to osteoblastic niche cells and, under normal conditions, maintains both the quiescence and enhanced survival of HSCs (1).

Although the hematopoiesis activity of LSK cells was not significantly different between the diabetic and nondiabetic mice, as measured by the colony-forming activity in the present study, the bone resorption activity of osteoclasts derived from hematopoietic progenitors (3) was abnormally increased